

Walking Gait Optimization for Accommodation of Unknown Terrain Height Variations

Brent Griffin and Jessy Grizzle

Abstract— We investigate the design of periodic gaits that will also function well in the presence of modestly uneven terrain. We use parameter optimization and, inspired by recent work of Dai and Tadrake, augment a cost function with terms that account for perturbations arising from a finite set of terrain height changes. Trajectory and control deviations are related to a nominal periodic orbit via a mechanical phase variable, which is more natural than comparing solutions on the basis of time. The mechanical phase variable is also used to penalize more heavily deviations that persist “late” into the gait. The method is illustrated both in simulation and in experiments on a planar bipedal robot.

I. INTRODUCTION

To be practical, bipedal robots must be able to walk over uneven terrain with imperfect knowledge of the ground profile. In this work, the gait design problem is formulated in terms of parameter optimization, with a cost function that accounts for periodicity under nominal walking conditions, and additional terms that specifically account for trajectory and control-effort perturbations arising from a finite set of ground height changes. When the method is evaluated on the planar biped shown in Fig. 1, for modest terrain height variations typical of sidewalks, parking lots, and maintained grass fields, it is observed that a cost function that favors *quasi dead-beat* rejection of terrain disturbances results in the best performing gaits of the three tested approaches, both in simulation and in experiments.

Numerous methodologies are being considered to quantify and improve the capacity of a bipedal robot to walk over uneven terrain. The terrain variations can be deterministic or random, and the control policy can involve switching or not. The gait sensitivity norm [1]–[3] has been used to measure deviations in state trajectories arising from unknown *step decreases* in ground height. Swing-leg retraction, employed by bipedal animals [4], has been observed to be helpful in accommodating this class of disturbances. The mean-time to falling has been used in [5] to assess walking performance in the presence of *stochastic ground height variations*. For low-dimensional dynamical systems, such as the rimless wheel and the compass bipedal walker, numerical dynamic programming has been used to maximize the mean time to falling. The simultaneous design of a periodic walking gait and a linear time-varying controller that minimizes deviations induced by ground height changes is addressed in [6], [7].

Brent Griffin and Jessy Grizzle are with the Department of Electrical Engineering and Computer Science, University of Michigan, Ann Arbor, MI 48109 USA e-mail: {griffb, grizzle}@umich.edu.

This work was supported by NSF grants ECCS-1343720 and ECCS-1231171.



Fig. 1: MARLO, an ATRIAS 2.1 robot designed by the Dynamic Robotics Laboratory at Oregon State University, walks with unknown terrain heights.

The results are illustrated through simulation on the compass gait biped and on Rabbit, a five-link biped with knees. A time-invariant linear controller that is robust to modest terrain variations is developed in [8], using transverse linearization and a receding-horizon control framework; experiments are performed on a compass-gait walker. An event-based controller is given in [9] that updates parameters in a fixed controller in order to achieve a *dead-beat control response*, in the sense that after a terrain disturbance, it steers the robot’s state back to its value at the end of the nominal periodic gait. A control architecture that *switches among a finite-set of controllers* when dealing with terrain variation is studied in [10], [11]. In the current paper, we seek a single (non-switching) controller and nominal periodic gait that are insensitive to a predetermined and finite set of terrain variations. This choice is motivated in part by ease of implementation, but even in the context of a switching controller, it seems desirable that one of the controllers be insensitive to a pre-determined range of terrain variation.

Motivated by the approach of Dai and Tadrake [6], [7], we seek a periodic walking gait that can accommodate a finite set of perturbations in ground height. Trajectory and control deviations induced by the perturbations are defined with respect to a nominal periodic orbit via a mechanical phase variable. As in [12], a parameterized family of *non-linear controllers* is assumed to be known and constrained parameter optimization is used to select a periodic solution of the closed-loop system that satisfies limits on torque, friction, and other physical quantities. Motivated by [6],

[7], the cost function is augmented with terms that penalize deviations in the state and control trajectories arising from the terrain perturbations. Two choices of cost function are studied. In one of them, the mechanical phase variable is used to penalize more heavily deviations that persist “late” into the gait while the other cost function makes no distinction of when the deviations occur. Focusing on deviations late in the gait is shown to improve the ability of the robot in Fig. 1 to handle terrain deviations, both in simulation and in experiments.

With respect to prior work on terrain variations, the primary contributions include:

- Allowing a family of nonlinear controllers to be searched over in the disturbance attenuation problem.
- Synchronizing the calculation of trajectory and control deviations of a biped’s gait via a mechanical phase variable.
- Penalizing more heavily trajectory deviations that persist late into a step, when ground contact is likely to occur.
- Illustrating in experiment the potential utility of trading off deviations early in the step for improved attenuation of the disturbance toward the end of the step.

II. WALKING MODEL AND SOLUTIONS

A. Hybrid Model

The walking model assumes alternating phases of single support (one foot on the ground) and double support (both feet in contact with the ground). The single support phase assumes the stance foot is not slipping and evolves as a passive pivot. The standard robot equations apply and give a second order model that is expressed in state variable form

$$\dot{x} = f(x) + g(x)u, \quad (1)$$

where $x \in \mathcal{X}$ is the state of the system and $u \in R^m$ are the control inputs. For later use, a parameterized family of continuous-time feedbacks is assumed to be given

$$u = \Gamma(x, \beta), \quad (2)$$

where $\beta \in \mathcal{B}$ are control parameters from an admissible set. The resulting closed-loop system is

$$\dot{x} = f^{cl}(x, \beta) := f(x) + g(x)\Gamma(x, \beta). \quad (3)$$

The closed-loop system is assumed to be continuously differentiable in x and β , thereby guaranteeing local existence and uniqueness of solutions.

With the stance foot taken as the origin let, p_2 be the Cartesian position of the swing foot on the second leg, and denote by p_2^v its vertical component. The double support phase occurs when the swing foot strikes the ground which is modeled as

$$p_2^v(x) - d = 0, \quad (4)$$

for $d \in D$, a finite collection of ground heights used to account for varying terrain. It will be assumed at impact that

the transversality condition $\dot{p}_2^v(x) < 0$ is met. Physically, it corresponds to the impact occurring at a point in the gait where the swing foot is moving down toward the ground, as opposed to the impact occurring early in the gait which would lead to tripping [11]. The impact is modeled as a collision of rigid bodies using the model of [13]. Consequently, the impact is instantaneous and gives rise to a continuously-differentiable reset map

$$x^+ = \Delta(x^-), \quad (5)$$

that does not depend on the ground height. Here, x^+ is a vector of the post-impact states and x^- is the vector of pre-impact states. So that only one continuous-phase mechanical model is needed, the impact map is assumed to include leg swapping, as in [12, pp. 57]. Moreover, for reasons that will become clear in Section IV, the impact map is allowed to depend on β .

The overall hybrid model is written as

$$\Sigma : \begin{cases} \dot{x} = f^{cl}(x, \beta) & x^- \notin \mathcal{S}^d \\ x^+ = \Delta(x^-, \beta) & x^- \in \mathcal{S}^d \end{cases} \quad (6)$$

where

$$d \in D := \{d_0, d_1, \dots, d_N\} \quad (7)$$

is the set of ground height variations and

$$\mathcal{S}^d := \{x \in \mathcal{X} \mid p_2^v(x) - d = 0, \dot{p}_2^v(x) < 0\} \quad (8)$$

is the hypersurface in the state space where the swing leg impact occurs at ground height $d \in D$.

Remark: The reference [12, pp. 109] shows how to augment the state variables with control parameters in order to accommodate event-based control, as used in [9]. This extension is employed later in (32).

B. Model Solutions

For a given value of $\beta \in \mathcal{B}$, a solution of the hybrid model (6) is defined by piecing together solutions of the differential equation (3) and the reset map (5); see [12, pp. 56], [13]. Because we are interested in periodic orbits and their perturbations, we exclude Zeno and other complex behavior from our notion of a solution.

In the following, for compactness of notation, explicit dependence on β is dropped. A *step* of the robot starts at time t_0 with $x_0 \in \mathcal{S}^{\bar{d}_0}$ for a given value of $\bar{d}_0 \in D$. The reset map is applied, giving an initial condition $\Delta(x_0)$ for the ODE (3), with solution $\varphi(t, t_0, \Delta(x_0))$. The step is completed if the solution of the ODE can be continued until a (first) time $t_1 > t_0$ when $x_1 = \varphi(t_1, t_0, \Delta(x_0)) \in \mathcal{S}^{\bar{d}_1}$ for a given value of $\bar{d}_1 \in D$. Not all steps can be completed, but when one is completed, the next step begins by solving the ODE with initial condition $\Delta(x_1)$ at time t_1 , etc. The solution (or step) is *periodic* if $\varphi(t_1, t_0, \Delta(x_0)) = x_0$, and $T = t_1 - t_0$ is the *period*. Because the model is time invariant, wherever convenient, the initial time is taken as $t_0 = 0$ and the solution denoted as $\varphi(t, \Delta(x_0))$.

III. OPTIMIZATION FOR ACCOMMODATION OF UNKNOWN TERRAIN DISTURBANCES

Let $d_0 \in D$ represent the nominal change in ground height *step to step*. We seek $\beta \in \mathcal{B}$ and $x_0 \in \mathcal{X}$ giving rise to a periodic solution of the closed-loop system (6); that is, for which there exists $T_0 > 0$ such that

$$x_0 = \varphi(T_0, \Delta(x_0)). \quad (9)$$

Moreover, for the same value of $\beta \in \mathcal{B}$, we desire that the periodic orbit ensures the existence of the following additional solutions of the closed-loop system: $\forall 1 \leq j \leq N$, $d_j \in D$, $\exists 0 < t_j < \infty$, and $0 < T_j < \infty$ such that

$$x_j := \varphi(t_j, \Delta(x_0)) \in \mathcal{S}^{d_j}, \quad (10)$$

and

$$\varphi(T_j, \Delta(x_j)) \in \mathcal{S}^{d_0}. \quad (11)$$

In plain words, there exist steps that begin on the periodic orbit, end at ground height d_j , and continue for at least one more step at nominal ground height d_0 .

In the following, we set up a parameter optimization problem in (β, x_0) for finding a periodic solution that meets these conditions. Moreover, we will pose a cost function on the steps following the change in ground height that favors solutions that “return closely” to the nominal periodic solution, that is, the closed-loop system attenuates the effects of the set of ground height variations.

A. Mechanical Phase and Trajectory Deviations

As in [6], [7], we have found that computing deviations of the perturbed solutions from the nominal periodic solution does not work well when the trajectories are parameterized by time. This is because terrain disturbances cause varying initial conditions, which cause perturbed trajectories to be unsynchronized with respect to time. We use instead a *mechanical phase* variable $\bar{\tau} : \mathcal{X} \rightarrow \mathbb{R}$ that is strictly increasing along walking steps. Examples include the horizontal position of the center of mass, the horizontal position of the hips, or the angle of the line connecting the hip and the ground contact point of the stance leg, which will be used in Section IV. The mechanical phase can be thought of as a measure of progress through each step. We further assume that the units are normalized on the periodic orbit so that it takes values in $[0, 1]$, namely

$$\bar{\tau}(\Delta(x_0)) = 0 \quad (12)$$

$$\bar{\tau}(x_0) = 1, \quad (13)$$

and that $L_g \bar{\tau}(x) := \frac{\partial \bar{\tau}}{\partial x}(x)g(x) = 0$.

Let $\bar{\tau}_j(t) := \bar{\tau}(\varphi(t, \Delta(x_j)))$, for $0 \leq t \leq T_j$, and as in [6], denote by τ_j^+ and τ_j^- the initial and final values of $\bar{\tau}$ along the trajectory. Due to the strictly increasing assumption, the inverse map $\bar{\tau}_j^{-1} : [\tau_j^+, \tau_j^-] \rightarrow [0, T_j]$ exists. Define

$$\tilde{x}_j(\tau) := \varphi(\bar{\tau}_j^{-1}(\tau), \Delta(x_j)) \quad (14)$$

$$\tilde{u}_j(\tau) := \Gamma(\varphi(\bar{\tau}_j^{-1}(\tau), \Delta(x_j)), \beta). \quad (15)$$

For $1 \leq j \leq N$, deviations in the state and control trajectories are defined as

$$\delta x_j(\tau) := \begin{cases} \tilde{x}_j(\tau) - \tilde{x}_0(0) & \text{if } \tau < 0 \\ \tilde{x}_j(\tau) - \tilde{x}_0(\tau) & \text{if } \tau \in [0, 1] \\ \tilde{x}_j(\tau) - \tilde{x}_0(1) & \text{if } \tau > 1 \end{cases} \quad (16)$$

$$\delta u_j(\tau) := \begin{cases} \tilde{u}_j(\tau) - \tilde{u}_0(0) & \text{if } \tau < 0 \\ \tilde{u}_j(\tau) - \tilde{u}_0(\tau) & \text{if } \tau \in [0, 1] \\ \tilde{u}_j(\tau) - \tilde{u}_0(1) & \text{if } \tau > 1 \end{cases} \quad (17)$$

for $\tau_j^+ \leq \tau \leq \tau_j^-$.

Using (16) and (17), the weighted square error is defined as

$$\|\delta x_j(\tau)\|^2 := \langle Q \delta x_j(\tau), \delta x_j(\tau) \rangle \quad (18)$$

$$\|\delta u_j(\tau)\|^2 := \langle R \delta u_j(\tau), \delta u_j(\tau) \rangle, \quad (19)$$

for Q and R positive semi-definite (constant) matrices.

B. Cost Function

The problem of defining a cost function \mathcal{J}_0 and appropriate equality and inequality constraints for determining a nominal periodic solution of (3) has been addressed in [12, pp. 151-155], [14], [15] using parameter optimization. Here we define additional terms that penalize deviations induced by the terrain height disturbances in D .

For $1 \leq j \leq N$, we define

$$\mathcal{J}_j = \frac{1}{(\tau_j^- - \tau_j^+)} \int_{\tau_j^+}^{\tau_j^-} (\|\delta x_j(\tau)\|^2 + \|\delta u_j(\tau)\|^2) \frac{(\tau - \tau_j^+)}{(\tau_j^- - \tau_j^+)} d\tau. \quad (20)$$

The term $\frac{(\tau - \tau_j^+)}{(\tau_j^- - \tau_j^+)}$ under the integral scales the errors so that initial deviations from the nominal periodic trajectory are discounted with respect to errors toward the end of the step. The rationale for this is that errors directly following the previous impact are much less problematic than errors that can compound at the following impact at the end of the step. The term $\frac{1}{(\tau_j^- - \tau_j^+)}$ outside the integral is included so that perturbed step costs are normalized w.r.t. the varying ranges of τ_j resulting from higher and lower terrain disturbances. The benefit of the scalings introduced in (20) will be illustrated by comparing control solutions that include them against those that do not.

The overall cost function is

$$\mathcal{J} = \mathcal{J}_0 + \sum_{j=1}^N w_j \mathcal{J}_j, \quad (21)$$

where w_j determines the relative weight of each perturbation.

Parameter optimization problem: Find $(\beta; x_0)$ that (locally) minimize \mathcal{J} subject to the existence of a periodic solution of (6) that respects ground contact conditions, torque limits, and other relevant physical properties, as illustrated in Section IV-(C).

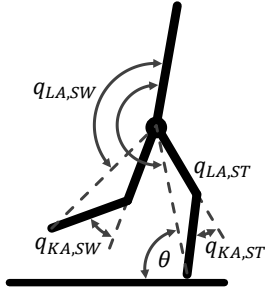


Fig. 2: State description for planar model of MARLO we use for simulation and control design.

IV. OPTIMIZATION IMPLEMENTATION

We now provide an implementation of the optimization approach for rejecting terrain disturbances presented in Section III.

A. Bipedal Robot MARLO

The robot used in this study, MARLO, is the Michigan copy of the ATRIAS-series of robots built by Jonathan Hurst [16]. The dynamic model is described in reference [17]. The robot's mass is approximately 55 kg and its legs are one meter long. Here, the robot is planarized through attachment to a boom. Furthermore, while the robot has series elastic actuators, the springs are stiff and in this study are removed from the model. With these simplifications, the robot has five DOF when in single support and four actuators.

The configuration variables are defined in Fig. 2. Specifically,

$$q = [\theta, q_{act}]', \quad (22)$$

where θ is the absolute angle of the stance leg clockwise from the horizontal plane at ground contact and

$$q_{act} = \begin{bmatrix} q_{LA,ST} \\ q_{LA,SW} \\ q_{KA,ST} \\ q_{KA,SW} \end{bmatrix} \quad (23)$$

is a vector of the actuated configuration variables. In (23), LA and KA are abbreviations of leg angle and knee angle, respectively, and ST and SW designate the stance and swing legs. The Lagrangian model for single support and the impact model are derived as in [17]. These models give rise to (1) and (5), with $x = (q; \dot{q}) \in \mathcal{X}$ an open subset of \mathbb{R}^{10} and $u \in \mathbb{R}^4$ for one degree of underactuation during single support.

B. Family of Feedback Controllers

The feedback controller is designed using the method of *virtual constraints* and *hybrid zero dynamics* [18], [19]. Briefly, a holonomic constraint that is expressed as an output and zeroed through the action of an actuator rather than the internal forces of a physical constraint is said to be *virtual*. Virtual constraints can be used to synchronize the links of a robot in order to achieve common objectives of walking, such as supporting the torso, advancing the swing leg in relation

to the stance leg, specifying foot clearance, etc. For planar MARLO, four virtual constraints are defined, one for each available actuator. The output vector y is defined in terms of the configuration variables and a set of parameters κ and β ,

$$y = h(q, \kappa, \beta), \quad (24)$$

in such a way that the output has vector relative degree 2 [20, pp. 220] on a subset of interest, $\mathcal{X} \times \mathcal{K} \times \mathcal{B}$. Specifically, κ is used to maintain *hybrid zero dynamics* following impacts with terrain disturbances. The feedback controller is based on input-output linearization, namely

$$u_{ff}(q, \dot{q}, \kappa, \beta) := -[L_g L_f h(q, \kappa, \beta)]^{-1} L_f^2 h(q, \dot{q}, \kappa, \beta), \quad (25)$$

$$u_{fb}(q, \dot{q}, \kappa, \beta) := -[L_g L_f h(q, \kappa, \beta)]^{-1} (K_p y + K_d \dot{y}), \quad (26)$$

with

$$u = \Gamma(q, \dot{q}, \kappa, \beta) := u_{ff}(q, \dot{q}, \kappa, \beta) + u_{fb}(q, \dot{q}, \kappa, \beta). \quad (27)$$

Along solutions of the closed-loop system,

$$\ddot{y} + K_d \dot{y} + K_p y \equiv 0. \quad (28)$$

Appendix A gives an explicit construction of $h(q, \kappa, \beta)$ in terms of the actuated variables q_{act} and a set of degree $(M+1)$ Bézier polynomials. Moreover, with this output choice, it is straightforward to construct a function $\Psi : \mathcal{S}^d \times \mathcal{B} \rightarrow \mathcal{K}$ such that for all

$$\beta \in \mathcal{B} \quad \text{and} \quad \begin{bmatrix} q^+ \\ \dot{q}^+ \end{bmatrix} = \Delta(q^-, \dot{q}^-)$$

the initial values of the outputs are zeroed, that is,

$$\begin{bmatrix} 0 \\ 0 \end{bmatrix} = \begin{bmatrix} y^+ \\ \dot{y}^+ \end{bmatrix} = \begin{bmatrix} h(q^+, \kappa^+, \beta) \\ \frac{\partial}{\partial q} h(q^+, \kappa^+, \beta) \dot{q}^+ \end{bmatrix} \quad (29)$$

for $\kappa^+ = \Psi(q^-, \dot{q}^-, \beta)$.

The parameters κ are constant within each step and are reset at the end of each step. They are thus formally states and are included in the dynamics with

$$x_e := [q, \dot{q}, \kappa]' \quad (30)$$

and $\dot{\kappa} = 0$. The closed-loop model used in the optimization is then

$$\Sigma : \begin{cases} \dot{x}_e = f^{cl}(x_e, \beta) & x_e^- \notin \mathcal{S}_e^d \\ x_e^+ = \Delta_e(x_e^-) & x_e^- \in \mathcal{S}_e^d, \end{cases} \quad (31)$$

where

$$f^{cl}(x_e, \beta) = f^{cl}(x, \kappa, \beta) := \begin{bmatrix} f(x) + g(x)\Gamma(x, \kappa, \beta) \\ 0 \end{bmatrix}, \quad (32)$$

$$\Delta_e(x_e^-, \beta) := \begin{bmatrix} \Delta(q^-, \dot{q}^-) \\ \Psi(q^-, \dot{q}^-, \beta) \end{bmatrix}, \quad (33)$$

and

$$\mathcal{S}_e^d := \mathcal{S}^d \times \mathcal{K}. \quad (34)$$

Remarks: (a) The reset map is independent of the current value of κ . (b) Because of the second-order system (28) and

the reset map in (29), solutions of (32) that are initialized in \mathcal{S}_e^d satisfy $y(t) \equiv 0$. This has two consequences: (i) The solutions evolve on the zero dynamics manifold, a 2-dimensional invariant surface and can thus be computed from a 2-dimensional vector field [19], [21]. This fact is used to accelerate the parameter optimization process. (ii) The feedback term u_{fb} in (26) is identically zero, and thus Γ in (27) is independent of the gains K_p and K_d .

C. Mechanical Phase and Three Periodic Orbits

Along periodic walking gaits, the coordinate θ shown in Fig. 2 is monotonic and cycles between a minimum value θ_{min} and a maximum value θ_{max} . The mechanical phase variable is defined as

$$\tau(x) = \frac{\theta - \theta_{min}}{\theta_{max} - \theta_{min}}. \quad (35)$$

The cost function for the nominal periodic orbit is taken as

$$\mathcal{J}_0 = \frac{1}{\text{step length}} \int_0^{T_0} \langle u, \dot{q}_{motor} \rangle dt, \quad (36)$$

where T_0 is the period, u is the 4-vector of motor torques, and \dot{q}_{motor} is the corresponding 4-vector of motor angular velocities, obtained from the link velocities and gear ratios [17]. The inner product of \dot{q}_{motor} and u is instantaneous mechanical power.

The nominal periodic orbit was computed for walking on level ground, that is $d_0 = 0$, by optimizing (36) subject to (32), and the following additional constraints: peak motor torque less than 2.5 Nm; vertical ground reaction force positive and friction coefficient less than 0.6; minimum foot clearance at mid-stance of 0.05 m; minimum knee bend of 22° to avoid hyperextension; average walking speed of at least 0.75 m/s; minimum swing-leg retraction of 7° ; dimensionless swing-leg retraction less than -0.5 [2]. The computations were performed with `fmincon` in MATLAB.

The set of terrain variations was taken as $D = \{0, \pm 2 \text{ cm}, \pm 4 \text{ cm}\}$. A second periodic gait was found that minimized the cost function (21), with $w_j = 100$ for $1 \leq j \leq 4$. Taking the weights all equal is analogous to assuming a uniform distribution of terrain variations [7].

To investigate the utility of discounting trajectory deviations that occur early in the perturbed steps, a third periodic orbit was found with the term $\frac{(\tau - \tau_j^+)}{(\tau_j^- - \tau_j^+)}$ removed from (20), resulting in

$$\mathcal{J}_j = \frac{1}{(\tau_j^- - \tau_j^+)} \int_{\tau_j^+}^{\tau_j^-} (||\delta x_j(\tau)||^2 + ||\delta u_j(\tau)||^2) d\tau. \quad (37)$$

In total, three gaits have been computed: a periodic gait that does not account for terrain variation and two that do. These will be denoted as Nominal, $NS_{4\text{cm}}$ and $S_{4\text{cm}}$, where the NS (not scaled) refers to the cost function (37) and S (scaled) refers to the cost function (20). In the next section, these gaits are evaluated both in simulation and experimentally.

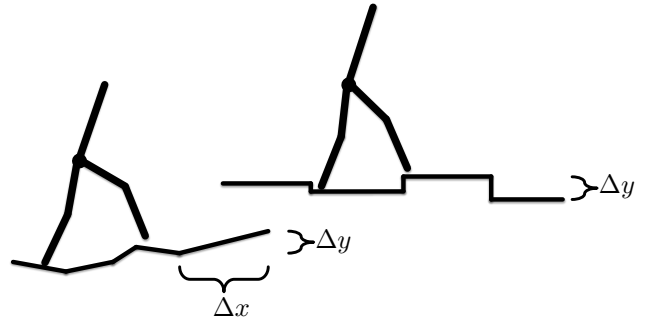


Fig. 3: Sloped (bottom left) and step (top right) terrain

V. RESULTS

The “raw” simulation and experimental results are given here, with discussion given in Section VI. Videos of the experiments are available at <http://youtu.be/OmhzbsCDN34> [22].

A. Simulations

1) *Control Law*: The simulations are conducted with the same controller that will be used in the experiments. Because the model of the robot is imperfect, even with the initialization (29), the outputs (24) (see also (38)) will not remain zero. Hence, the feedback term (26) is used with $K_p = (\frac{1}{0.03})^2$ and $K_d = 60$. Due to the 50:1 gear ratio of the harmonic drives, the feedforward term (25) is not essential and is dropped, as in [14]. The parameter update portion of the reset map (29) is pre-computed and interpolated using $\tau(x^+)$ of each step.

2) *Terrain and Results*: Two types of terrain profiles were generated, stepped and sloped, as shown in Fig. 3. Step-terrain profiles consist of one vertical displacement per step, modeled as an i.i.d. uniform random variables with $-4 \text{ cm} \leq d \leq 4 \text{ cm}$. Fifty such terrains were generated, each with a length of 10,000 steps. The sloped terrain is meant to more closely approximate real ground variation. It uses an additional i.i.d. uniform random variables to determine the horizontal intervals between vertical displacements. Because the average step length of the three periodic gaits was approximately 0.5 m, the horizontal intervals are chosen uniformly between 0.25 m and 0.75 m. Because the intervals between height changes are random, it is possible to have more than one vertical displacement in the span of a single walking step. As a result, the sloped-terrain profile admits disturbances that exceed 4 cm over a single step. Fifty sloped terrains were generated, each long enough that at least 10,000 steps would be possible.

Each of the three gaits was evaluated over each of the 100 terrain profiles, 50 stepped and 50 sloped. A simulation over a given terrain profile was initiated at the gait’s fixed-point and terminated when the robot reached 10,000 steps or fell. A fall could occur from losing momentum and falling backward, gaining too much momentum and falling forward, or slipping after violating ground contact constraints. The results of these simulations are summarized in Table I.

TABLE I: Simulation results for all control solutions.

Control	Number of Steps					Finished Trials
	Mean ^a	Med.	Min.	Max.	Variation Coef.	
4 cm Step Terrain						
Nominal	192	112	6	1157	1.22	0
NS_{4cm}	85	67	5	404	0.96	0
S_{4cm}	4616	4499	165	10^4	0.73	4
4 cm Sloped Sidewalk						
Nominal	481	331	17	2224	0.93	0
NS_{4cm}	218	178	15	740	0.79	0
S_{4cm}	4543	3335	40	10^4	0.71	8

^a S_{4cm} mean could be higher, but trials were limited to 10,000 steps.

TABLE II: Cost function \mathcal{J}_0 evaluated on periodic terrain with constant step height changes.

Constant Step Disturbance	Periodic Efficiency (J/m) ^a		
	Nominal	NS_{4cm}	S_{4cm}
3 cm	Unstable	Unstable	58.5
2 cm	41.2	42.4	55.7
0 cm	35.6	39.6	52.5
-2 cm	35.2	37.8	48.4
-4 cm	42.3	36.0	39.7

^aPeriodic efficiency is calculated using (36).

An additional set of simulations over terrain with periodic, constant stepped height changes was performed and the cost function \mathcal{J}_0 in (36) was evaluated. The results are in Table II.

B. Robot Experiments

1) *Experiment Setup*: The robot MARLO with point feet is attached to a 2.4 m boom to impose a planar gait. The center of the boom is mounted near a wall of the laboratory, and hence the maximum distance of an experiment is 7.5 m. Because the robot is walking in a circle, the outside leg travels a longer distance than the inside leg. To partially compensate for this, in the last 25% of a gait, the lateral hip angles are commanded to move the feet toward the center of the robot; to avoid leg collisions, the legs are moved outward toward the middle of the gait.

A terrain of variable height is constructed by stacking sections of plywood that are approximately 61 cm long [23, Fig. 25]. The plywood terrain is then overlaid with rubber mats to increase friction. Each experiment is initiated from a static pose with the robot’s CoM a few millimeters in front of the stance leg. Each terrain begins with a few steps downward so that the transfer of potential energy to kinetic energy will cause the robot to quickly transition from zero velocity to approximately its velocity on the periodic orbit.

2) *Experiment Results*: When a fall occurred in the simulations, it was only after consecutive uphill steps. We thus set up an uphill terrain, shown in Fig. 4, to compare the Nominal, NS_{4cm} , and S_{4cm} gaits. Each of the three gaits was executed over the uphill terrain three times for nine total trials, as shown in Table III. The S_{4cm} controller was able to complete all three trials with a consistent walking speed, as shown in Fig. 5. The Nominal controller was able

TABLE III: Experimental results for all control solutions. Three consecutive trials are performed for each controller on the Uphill Terrain depicted in Figure 4. S_{4cm} is the only controller to complete the terrain on all three trials.

Control	Number of Steps			Stalls	Falls	Finished Trials
	Trial 1	Trial 2	Trial 3			
Uphill Terrain						
S_{4cm}	12	12	12	0	0	3
Nominal	12	12	7	1	0	2
NS_{4cm}	7	6	7	2	1	0

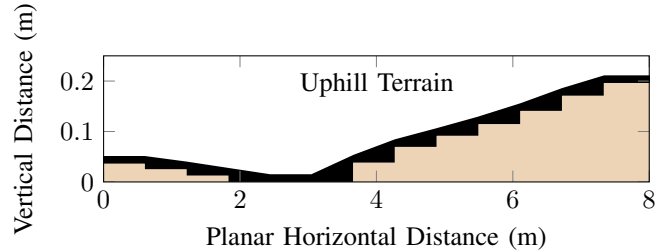


Fig. 4: Planar view of experimental terrain we use for comparing control. Stair height is accurate (brown), while the rubber mats heights are approximate (black).

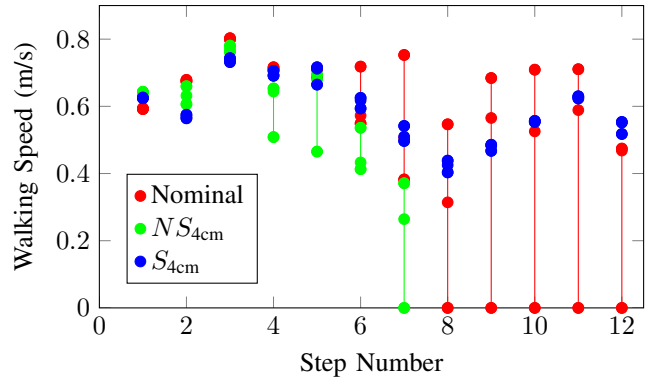


Fig. 5: Walking speed vs. step number for all Uphill Terrain experiments. Lines connect data for each control from maximum to minimum speeds. Data points for incomplete steps are set at zero.

to complete the terrain course twice, but stalled¹ during one trial. The NS_{4cm} controller was not able to complete the terrain on any trials due to stalling on two trials and falling on one.

In the next set of experiments, the S_{4cm} gait was further evaluated over the terrains illustrated in Fig. 6. We performed consecutive completed trials for each terrain. The results are documented in the video [22]. Height changes for experimental terrains are given in Table IV.

VI. DISCUSSION

Table V presents the minimum angular momentum about the stance leg over the step following a terrain perturbation

¹A stall occurs when the robot lacks adequate momentum to complete a step, and thus settles backward onto the previous stance leg rather than transition to the next step.

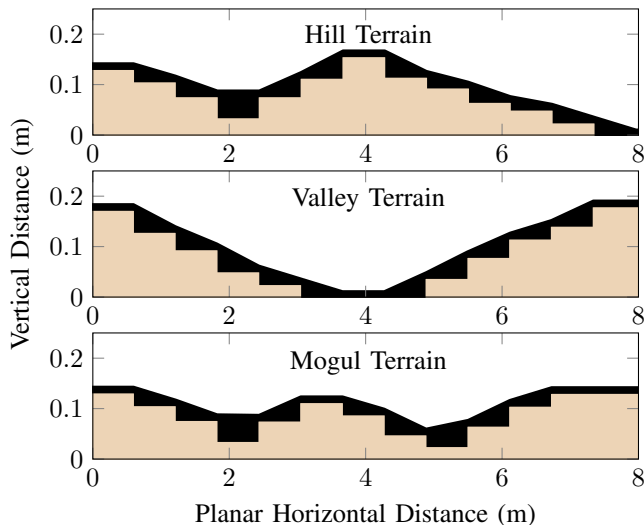


Fig. 6: Additional experimental terrain for $S_{4\text{cm}}$.

TABLE IV: Height changes between wood steps for experimental terrains. Distance between steps is approximately 61 cm.

Terrain	Height Changes (cm)
Uphill	-1.1, -1.25, -1.25, 0, 0, 3.8, 3.1, 2.2, 2.3, 2.6, 3, 2.5
Hill	-2.4, -2.9, -4.1, 4.1, 3.6, 4.2, -4, -2.1, -2.8, -1.5, -2.5, -2.5
Valley	-4.3, -3.4, -4.3, -2.5, -2.5, 0, 0, 3.7, 4.1, 3.6, 2.5, 3.8
Mogul	-2.5, -2.9, -4.1, 4, 3.6, -2.4, -3.9, -2.3, 4, 3.9, 2.5

TABLE V: Minimum angular momentum about the stance foot and impact losses for perturbed steps in optimization.

d	Minimum Angular Momentum (Nms)			Impact Losses (J)		
	Nominal	$NS_{4\text{cm}}$	$S_{4\text{cm}}$	Nominal	$NS_{4\text{cm}}$	$S_{4\text{cm}}$
4 cm	40.5	38.3	43.8	8.3	10.1	13.9
0 cm	54.4	54.7	53.5	17.8	18.8	24.6
-4 cm	53.0	52.3	54.6	50.4	47.4	39.2

of height $d_i \in D$. The $S_{4\text{cm}}$ gait maintains on average greater angular momentum at peak potential energy than the other gaits. Furthermore, with a single 4 cm disturbance the minimum angular momentum of the Nominal and $NS_{4\text{cm}}$ gaits decreases 26% and 30% respectively, while the $S_{4\text{cm}}$ gait decreases 18%. In simulation, we found falling backward after losing momentum from repeated uphill disturbances to be the only failure mode. Having a more reliable reserve of angular momentum explains in part why the $S_{4\text{cm}}$ gait was able to outperform the other gaits in simulation and experiments (Tables I & III).

Because consecutive uphill steps led to every fall in the simulations, the initial experiments focused on comparing all controllers on the uphill terrain of Fig. 4. The Nominal and $NS_{4\text{cm}}$ gaits were unreliable. The lower and less consistent swing foot trajectories in Fig. 7 are prone to scuffing and premature impacts, both of which inhibit a consistent forward velocity (Fig. 5). The $S_{4\text{cm}}$ gait exhibited much better disturbance attenuation in terms of swing foot trajectory and speed. However, a consequence of the $S_{4\text{cm}}$ gait's higher swing foot

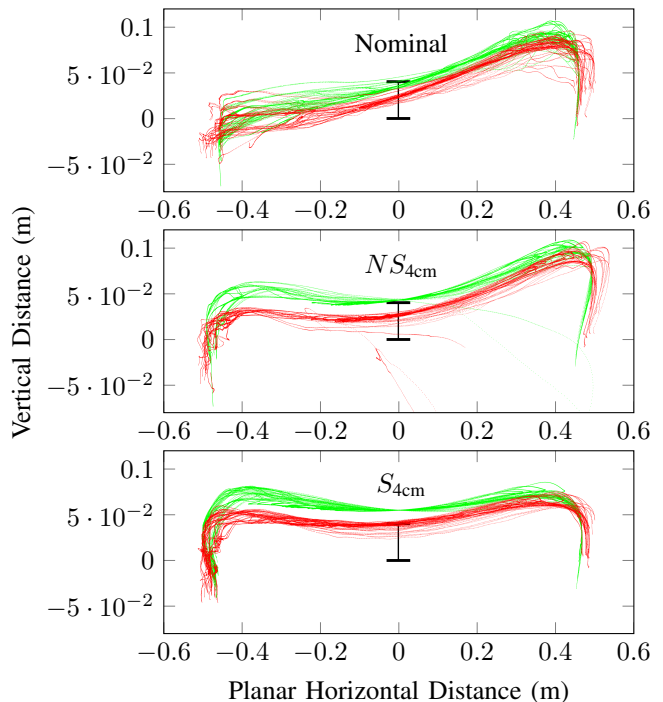


Fig. 7: Actual (Red) and desired (Green) swing foot trajectories relative to stance foot. Top black bar on each plot indicates 4 cm above the origin or stance foot position for each trajectory. Plots generated using data from all Uphill Terrain experiments, hence, the swing foot starts below the stance foot for some trajectories.

clearance is a higher impact loss on flat ground (Table V).

Table II shows that the Nominal gait is the most energy efficient for flat terrain. However, with some disturbances the other two gaits are more energy efficient than the Nominal gait. Hence, the advantages of the Nominal gait are dependent on avoiding terrain disturbances, which may be inconsistent with outdoor operation. As emphasized in [24], efficiency may be out-weighted by robustness.

Overall, the $S_{4\text{cm}}$ gait outperformed the $NS_{4\text{cm}}$ gait. We believe that allowing the optimizer to accept actions in the beginning of the step that resulted in smaller errors later in the step, near the moment of impact, is the main reason for this. The difference between the $S_{4\text{cm}}$ and $NS_{4\text{cm}}$ optimizations was the use of scaling variables in the $S_{4\text{cm}}$ to emphasize end-of-step errors. This gait was shown to work well in a variety of environments.

APPENDIX I BÉZIER PARAMETER RESET DERIVATION

In Section IV, we discuss how control parameters κ must be reset such that we satisfy (29). First, we define our output

$$y = h(q, \kappa, \beta) = q_{act}(q) - h_d(q, \kappa, \beta), \quad (38)$$

where $h_d \in \mathbb{R}^4$ are desired trajectories defined by Bézier polynomials. Each i th polynomial is defined as

$$h_{d,i}(q, \kappa, \beta) := \sum_{k=0}^M \alpha_{i,k} \frac{M!}{k!(M-k)!} \tau^k (1-\tau)^{M-k}. \quad (39)$$

A set of four degree $(M+1)$ Bézier polynomials can be defined by $\alpha \in \mathbb{R}^{4 \times (M+1)}$ [12, pp. 138]. We designate the first two columns of parameters, α_0 and α_1 , as κ . α_0 and α_1 have the most effect on trajectories immediately after impact during low τ values. The remaining fixed columns, β , determine trajectories toward the end of the gait. Hence, perturbed steps return to the nominal gait as τ increases.

Let $y^+ = \dot{y}^+ = 0$ as in (29). Using (38), this implies that

$$h_d(q^+, \kappa^+, \beta) = q_{act}^+. \quad (40)$$

Note, to match h_d to q_{act}^+ , we must reset at least one column of Bézier parameters. To guarantee desired trajectories match post-impact velocities, we reset a second column to satisfy

$$\frac{\partial h_d(q^+, \kappa^+, \beta)}{\partial \tau} \dot{\tau}^+ = \dot{q}_{act}^+. \quad (41)$$

Solving (40) and (41) using α_0 and α_1 we find

$$\alpha_0 = \frac{q_{act}^+ - \sum_{k=1}^M \alpha_k \frac{M!(\tau^+)^k (1-\tau^+)^{M-k}}{k!(M-k)!}}{(1-\tau^+)^M} \quad (42)$$

$$\alpha_1 = \frac{\frac{\dot{q}_{act}^+}{\dot{\tau}^+} - \alpha_2 M(M-1)\tau^+(1-\tau^+)^{M-2} - a + b}{M((1-\tau^+)^{M-1} + \tau^+(1-\tau^+)^{M-2})} \quad (43)$$

$$a = \sum_{k=2}^{M-1} (\alpha_{k+1} - \alpha_k) \frac{M!(\tau^+)^k (1-\tau^+)^{M-1-k}}{k!(M-1-k)!} \quad (44)$$

$$b = \frac{M}{1-\tau^+} \left(q_{act}^+ - \sum_{k=2}^M \alpha_k \frac{M!(\tau^+)^k (1-\tau^+)^{M-k}}{k!(M-k)!} \right), \quad (45)$$

which is a solution for κ^+ that always satisfies (29).

ACKNOWLEDGMENT

Gabriel Buche, Brian Buss, and Xingye Da are sincerely thanked for their contributions to the experiments. Jonathan Hurst and his team at Oregon State University designed the robot.

REFERENCES

- [1] D. G. E. Hobbelen and M. Wisse, "A disturbance rejection measure for limit cycle walkers: The gait sensitivity norm," *Robotics, IEEE Transactions on*, vol. 23, no. 6, pp. 1213–1224, 2007.
- [2] —, "Swing-leg retraction for limit cycle walkers improves disturbance rejection," *Robotics, IEEE Transactions on*, vol. 24, no. 2, pp. 377–389, 2008.
- [3] M. Wisse, A. L. Schwab, R. Q. van der Linde, and F. C. T. van der Helm, "How to keep from falling forward: Elementary swing leg action for passive dynamic walkers," *IEEE Trans. on Robotics*, vol. 21, no. 3, pp. 393–401, June 2005.
- [4] A. Seyfarth, H. Geyer, and H. Herr, "Swing leg retraction: A simple control model for stable running," *Journal of Experimental Biology*, vol. 206, pp. 2547–2555, 2003.
- [5] K. Byl and R. Tedrake, "Metastable walking machines," *The International Journal of Robotics Research*, vol. 28, no. 8, pp. 1040–1064, 2009.
- [6] H. Dai and R. Tedrake, "Optimizing robust limit cycles for legged locomotion on unknown terrain," in *Decision and Control (CDC), 2012 IEEE 51st Annual Conference on*, 2012, pp. 1207–1213.
- [7] —, "L2-gain optimization for robust bipedal walking on unknown terrain," in *Robotics and Automation (ICRA), 2013 IEEE International Conference on*, 2013.
- [8] I. R. Manchester, U. Mettin, F. Iida, and R. Tedrake, "Stable dynamic walking over uneven terrain," *The International Journal of Robotics Research*, pp. 265–279, 2011.
- [9] S. Kolathaya and A. D. Ames, "Achieving bipedal locomotion on rough terrain through human-inspired control," in *Safety, Security, and Rescue Robotics (SSRR), 2012 IEEE International Symposium on*. IEEE, 2012, pp. 1–6.
- [10] T. Yang, E. Westervelt, A. Serrani, and J. P. Schmedeler, "A framework for the control of stable aperiodic walking in underactuated planar bipeds," *Autonomous Robots*, vol. 27, no. 3, pp. 277–290, 2009.
- [11] H. W. Park, "Control of a bipedal robot walker on rough terrain," Ph.D. dissertation, University of Michigan, 2012.
- [12] E. R. Westervelt, J. W. Grizzle, C. Chevallereau, J. Choi, and B. Morris, *Feedback Control of Dynamic Bipedal Robot Locomotion*, ser. Control and Automation. Boca Raton, FL: CRC Press, June 2007.
- [13] Y. Hürmüzli and D. B. Marghitu, "Rigid body collisions of planar kinematic chains with multiple contact points," *International Journal of Robotics Research*, vol. 13, no. 1, pp. 82–92, 1994.
- [14] E. R. Westervelt, G. Buche, and J. W. Grizzle, "Experimental validation of a framework for the design of controllers that induce stable walking in planar bipeds," *International Journal of Robotics Research*, vol. 24, no. 6, pp. 559–582, June 2004.
- [15] K. Sreenath, H. Park, I. Poulakakis, and J. Grizzle, "A compliant hybrid zero dynamics controller for stable, efficient and fast bipedal walking on MABEL," *International Journal of Robotics Research*, vol. 30(9), pp. 1170–1193, 2011.
- [16] J. Grimes and J. Hurst, "The design of ATRIAS 1.0 a unique monopod, hopping robot," *Climbing and walking Robots and the Support Technologies for Mobile Machines, International Conference on*, 2012.
- [17] A. Ramezani, J. W. Hurst, K. A. Hamed, and J. Grizzle, "Performance analysis and feedback control of atrias, a three-dimensional bipedal robot," *Journal of Dynamic Systems, Measurement, and Control*, vol. 136, no. 2, 2014.
- [18] J. W. Grizzle, G. Abba, and F. Plestan, "Asymptotically stable walking for biped robots: Analysis via systems with impulse effects," *IEEE Transactions on Automatic Control*, vol. 46, pp. 51–64, January 2001.
- [19] E. R. Westervelt, J. W. Grizzle, and D. E. Koditschek, "Hybrid zero dynamics of planar biped walkers," *IEEE Transactions on Automatic Control*, vol. 48, no. 1, pp. 42–56, Jan. 2003.
- [20] A. Isidori, *Nonlinear Control Systems*, 3rd ed. Berlin: Springer-Verlag, 1995.
- [21] B. Morris and J. W. Grizzle, "Hybrid invariant manifolds in systems with impulse effects with application to periodic locomotion in bipedal robots," *IEEE Transactions on Automatic Control*, vol. 54, no. 8, pp. 1751–1764, August 2009.
- [22] B. Griffin and J. Grizzle, "Walking gait optimization for accommodation of unknown terrain height variations. Youtube Video: <http://youtu.be/OmhzbsCDN34>.
- [23] H.-W. Park, K. Sreenath, J. W. Hurst, and J. W. Grizzle, "Identification of a bipedal robot with a compliant drivetrain," *IEEE Control Systems Magazine*, vol. 31, no. 2, pp. 63–88, April 2011.
- [24] C. O. Saglam and K. Byl, "Quantifying the trade-offs between stability versus energy use for underactuated biped walking," in *IEEE/RSJ International Conference on Intelligent Robots and Systems*. IEEE, Sep. 2014.